Science Advances

www.advances.sciencemag.org/cgi/content/full/1/4/e1500169/DC1

Supplementary Materials for

Activation of GTP hydrolysis in mRNA-tRNA translocation by elongation factor G

Wen Li, Zheng Liu, Ravi Kiran Koripella, Robert Langlois, Suparna Sanyal, Joachim Frank

Published 22 May 2015, *Sci. Adv.* **1**, e1500169 (2015)
DOI: 10.1126/sciadv.1500169

The PDF file includes:

Fig. S1. Gallery of four cryo-EM maps obtained by classification.
Fig. S2. Examples for map fittings.
Fig. S3. Density for GTP in the nonrotated complex.
Fig. S4. Interaction of protein S12 with domain III.
Fig. S5. Densities linking domain III to IV and domain II to V in our maps.
Fig. S6. Three-stage (I, II, III) classification of the entire data set using RELION.
Fig. S7. Color code for the resolution values in the movie showing the local resolution map.
Legends to movies S1 to S3

Other Supplementary Material for this manuscript includes the following:
(available at www.advances.sciencemag.org/cgi/content/full/1/4/e1500169/DC1)

Movie S1 (.mov format). Overview and local resolution estimation for the 3.6-Å map.
Movie S2 (.mov format). Examples of high-resolution protein features in the 3.6-Å map.
Movie S3 (.mov format). Examples of high-resolution RNA features in the 3.6-Å map.

Supplementary Information

Fig. S1. Gallery of four cryo-EM maps obtained by classification. (A) EF-G-bound non-rotated complex. (B). EF-G-unbound non-rotated complex. (C). EF-G-bound rotated complex. (D). EF-G-unbound rotated complex (see Table 1 for more detailed information on how these maps were obtained).

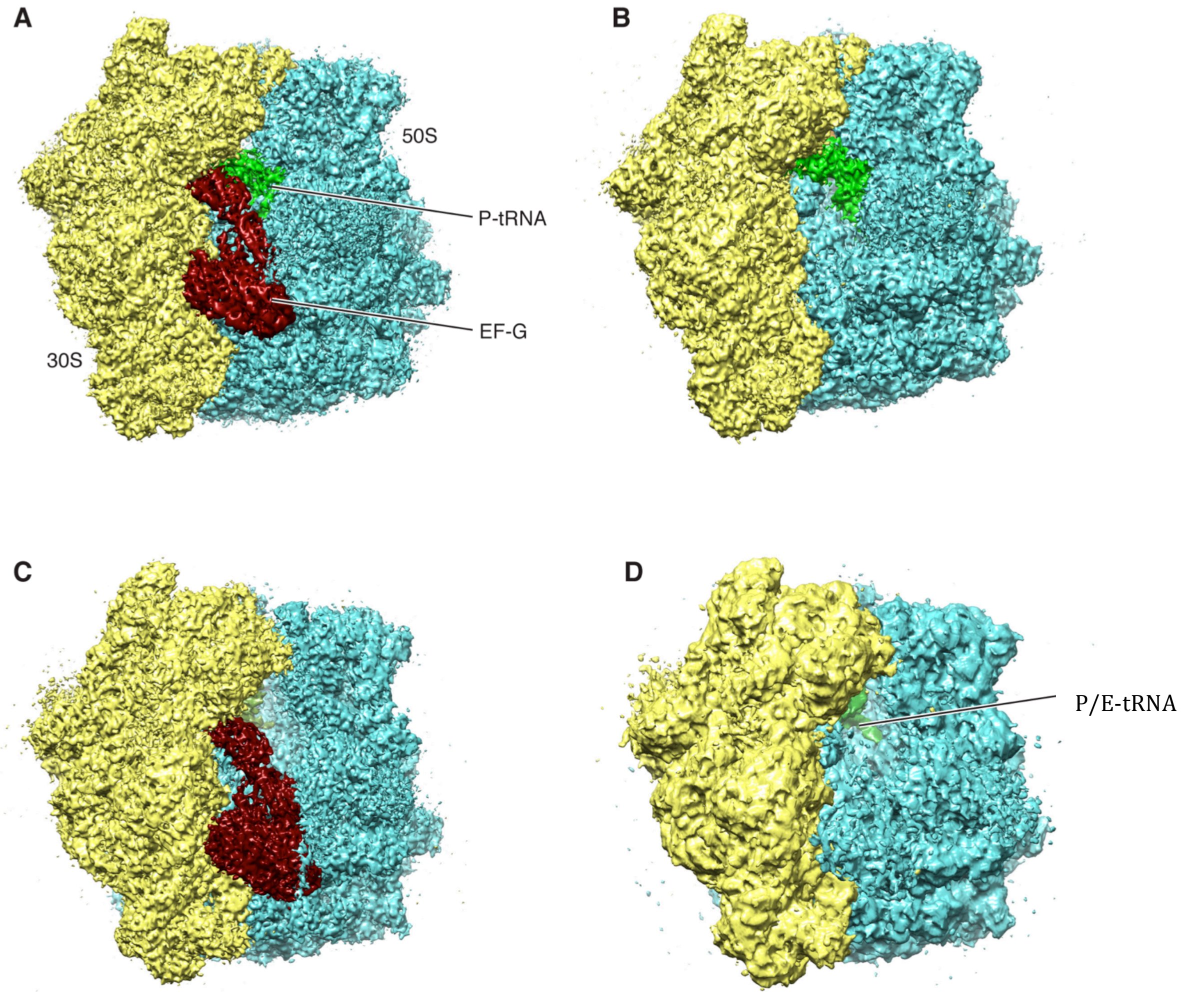

Fig. S2. Examples for map fittings. (A) A helical region in protein L20 in the map of the non-rotated EF-G-bound complex (Fig. 3A). The map is shown as grey mesh. (B) Density (mesh) for nucleotides 1604-1623 in 23S rRNA in the same complex.

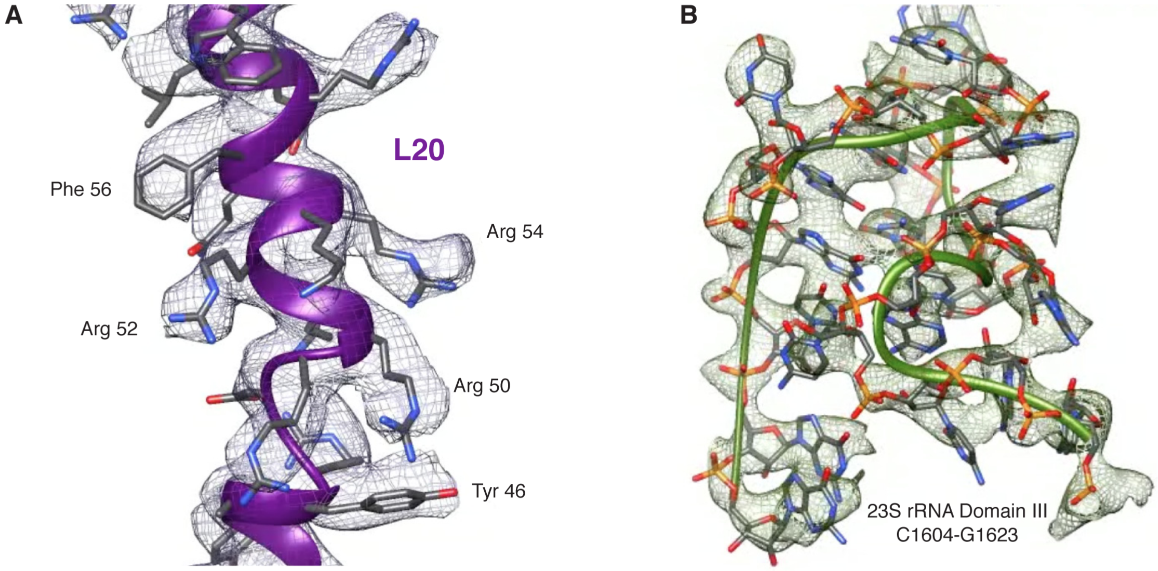

Fig. S3. Density for GTP in the non-rotated complex. (A) The map segment (mesh) for EF-G in the non-rotated complex, fitted with the structural model (yellow). (B) Density map in (A), displayed at a high threshold to show the density around GTP, the region boxed in (A). (See also Fig. 5 for the rotated complex).

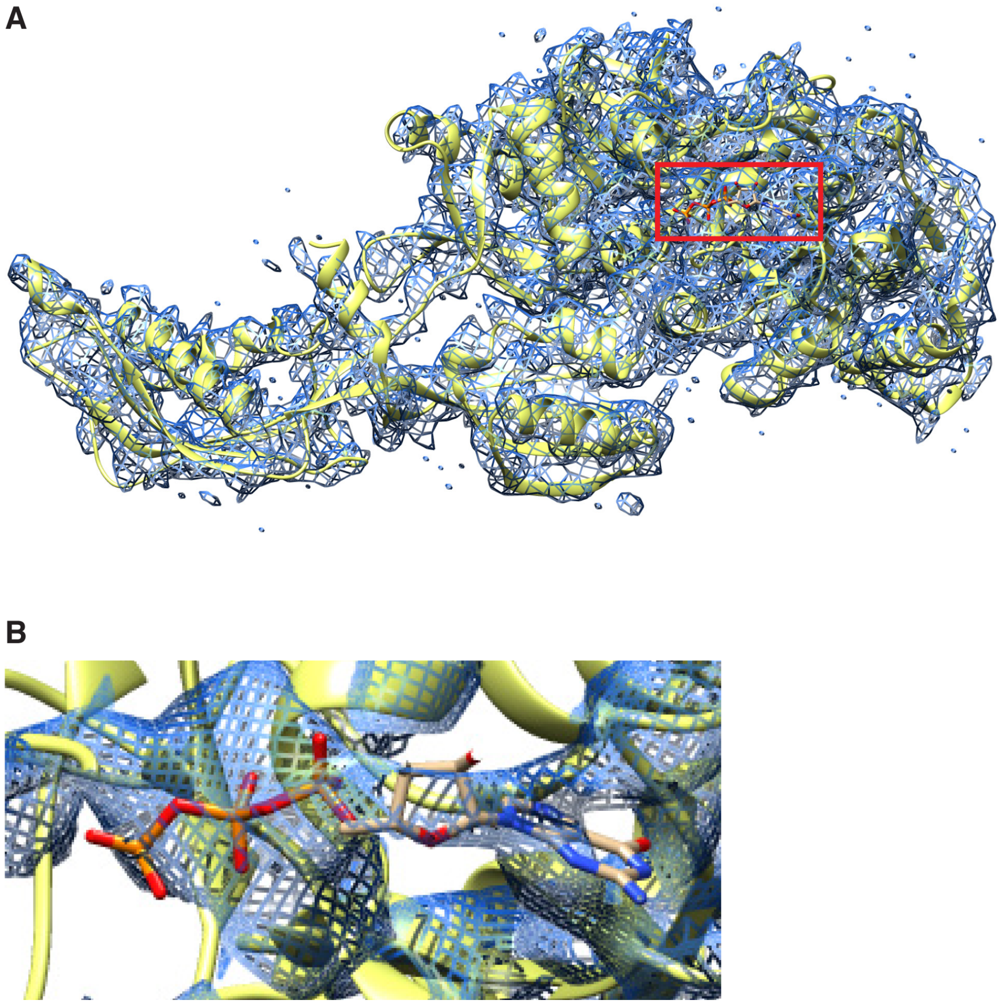

Fig. S4. Interaction of protein S12 with domain III. (A) S12's insertion into domain III of EF-G in a representative X-ray structure of PRE complex (orange; PDB code: 4BTC) vs. the structure in the non-rotated map (purple). Domains I and II in these two structures are superimposed. (B) The X-ray structure shown in (A) vs. the structure in the rotated map (dark green). (C) S12's insertion is also seen in the X-ray post-translocational complex (limegreen; PDB code: 2WRI), similarly to the X-ray PRE structure (orange) shown in (A). (D) Zoomed-in view of the region boxed in (C).

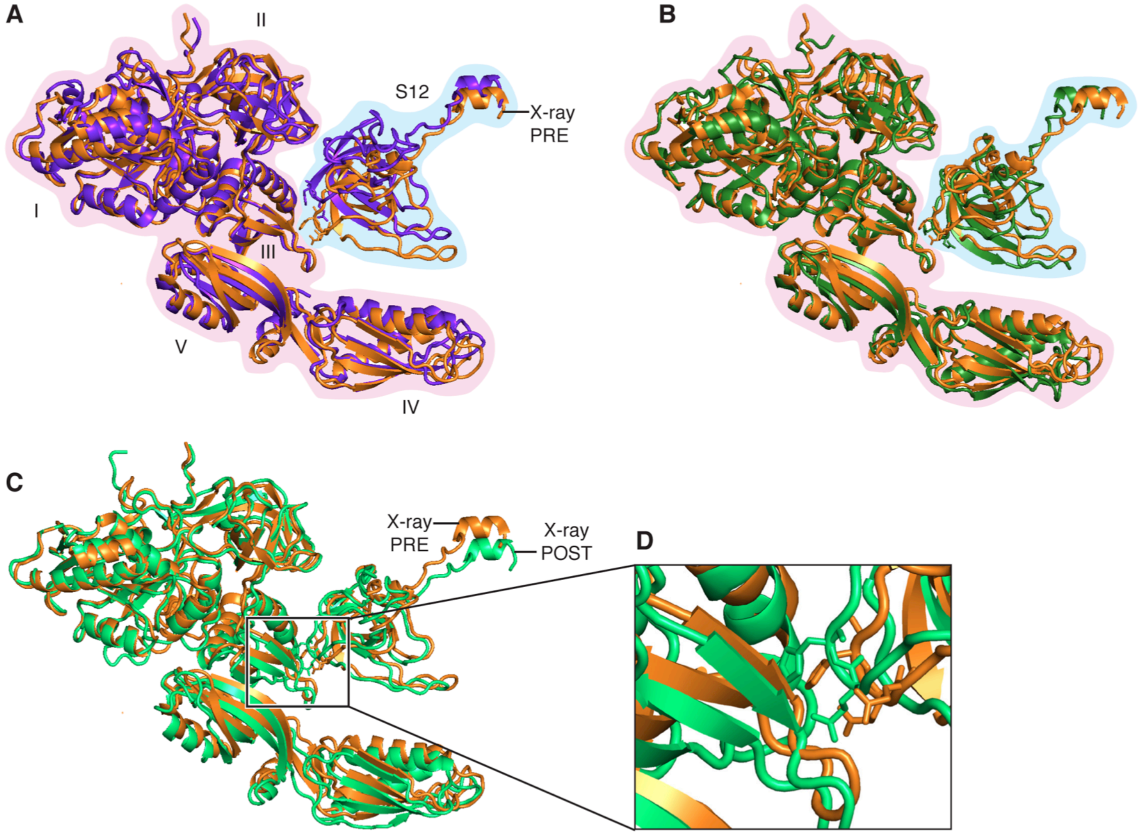

Fig. S5. Densities linking domain III to IV, and domain II to V in our maps. Maps displayed at a threshold level of three standard deviations. (A) Non-rotated complex. (B) Rotated complex.

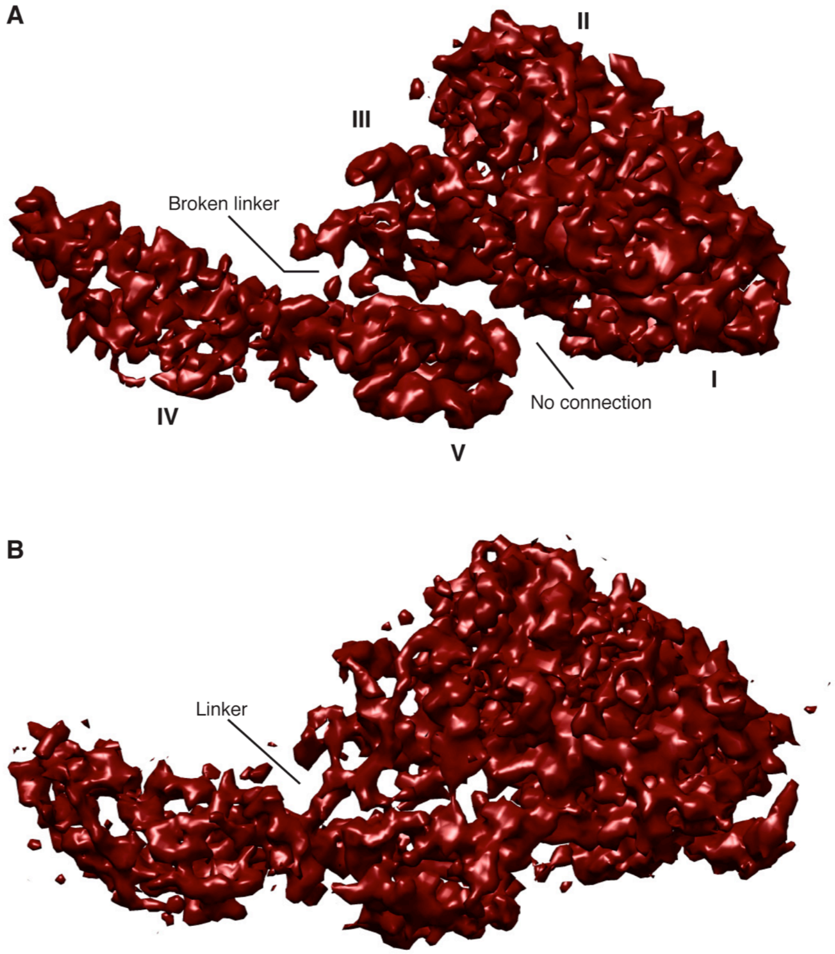

Fig. S6. Three-stage (I, II, III) classification of the entire data set using RELION. Each class is represented by the reconstruction from particles falling in that class.

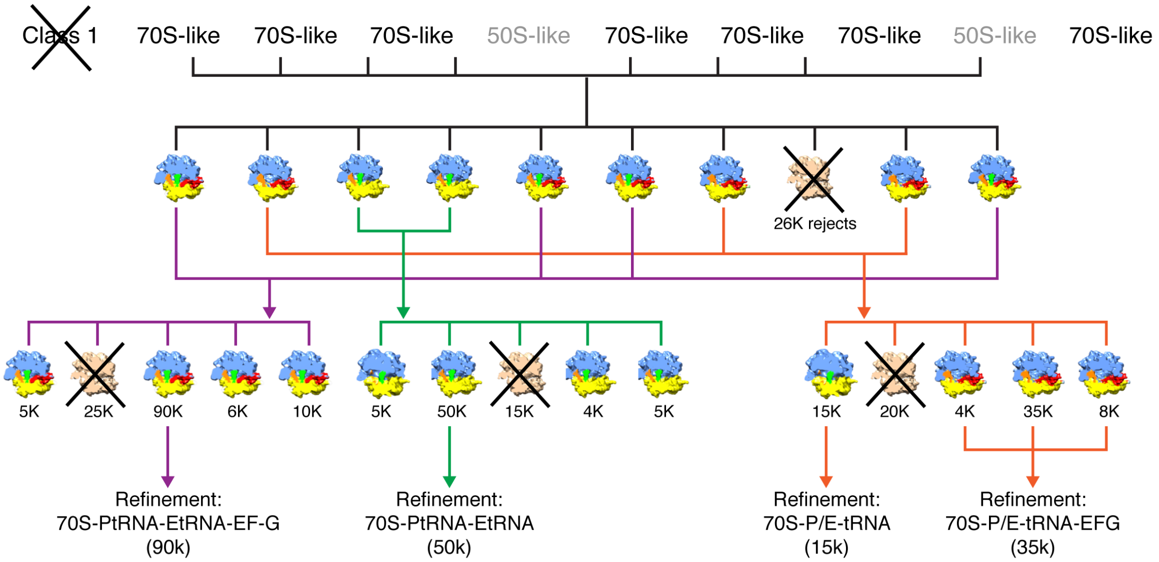

Fig. S7. Color code for the resolution values in the movie showing the local resolution map.

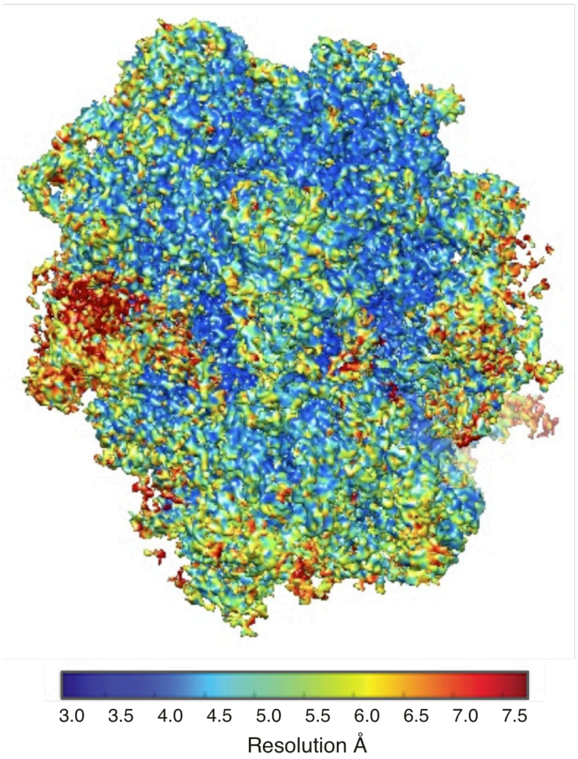

Movie S1. Overview and local resolution estimation for the 3.6 Å map. See color bar in Fig. S7.

Movie S2. Examples of high-resolution protein features in the 3.6 Å map.

Movie S3. Examples of high-resolution RNA features in the 3.6 Å map.